NMC Case Report Journal 9, 101-109, 2022

Clinicopathological and Genomic Features of Pediatric Intracranial Myxoid Mesenchymal Tumor with both of EWSR1-CREM Gene Fusion and MAP3K13 Mutation: A Case Report and Comparison with Adult Cases in the Literature

Minami SASAKI,[1] Seiichiro HIRONO,[1] Yue GAO,[1] Izumi SUDA,[1]
Tomoo MATSUTANI,[1] Masayuki OTA,[2] Takashi KISHIMOTO,[3] Jun-Ichiro IKEDA,[2]
Hideaki YOKOO,[4] and Yasuo IWADATE[1]

[1]*Department of Neurological Surgery, Chiba University Graduate School of Medicine, Chiba, Chiba, Japan*
[2]*Department of Diagnostic Pathology, Chiba University Graduate School of Medicine, Chiba, Chiba, Japan*
[3]*Department of Molecular Pathology, Chiba University Graduate School of Medicine, Chiba, Chiba, Japan*
[4]*Department of Human Pathology, Gunma University Graduate School of Medicine, Maebashi, Gunma, Japan*

Abstract

Intracranial myxoid mesenchymal tumors (IMMTs) with *EWSR1-CREB1* family gene fusion are rare brain neoplasms characterized by gene fusion between the *EWSR1* gene and one of the cyclic AMP response element-binding (CREB) family transcription factor (*CREB1*, *ATF1*, or *CREM*) genes. Although half of reported cases are pediatric, the clinical, histologic, and genomic features of IMMTs with *EWSR1* rearrangement in pediatric populations are not yet well clarified. Here we describe the case of a 7-year-old girl who presented with seizures due to an extra-axial tumor in the left parietal convexity. Gross total resection was achieved, and the tumor displayed a multilobular structure with solid hypercellular and myxoid hypocellular areas, separated by a variable amount of stroma. The hypercellular areas consisted of round to polygonal cells, whereas the myxoid areas were ovoid to spindled cells. Immunophenotypically, the tumor cells were positive for vimentin, desmin, and EMA. Next-generation sequencing of tumoral DNA revealed *EWSR1-CREM* gene fusion and a pathogenic mutation of *MAP3K 13*. No recurrence was detected 9 months after resection, without chemotherapy or radiotherapy. In comparison to other pediatric and adult patients with *EWSR1* rearrangement, many clinical, radiological, and immunohistochemical features were shared. However, signs of elevated intracranial pressure were more frequently observed, and postoperative radiation was less frequently administered for pediatric patients. Gross total resection (GTR) was the key prognostic factor for better disease control especially among pediatric patients. Further reports of cases with *EWSR1* rearrangement with detailed genetic profiles are essential for clarifying the oncogenic pathway and establishing a standard treatment strategy.

Keywords: pediatric, intracranial mesenchymal tumor, EWSR1, MAP3K13, gene fusion

Introduction

Intracranial myxoid mesenchymal tumors (IMMTs) harboring *EWSR1* (Ewing sarcoma breakpoint region 1) gene rearrangement, first reported in 2008 by Dunham et al.[1)] as an intracerebral angiomatoid fibrous histiocytoma (AFH), are rare brain neoplasms that are genetically defined by gene fusions between *EWSR1* and one of the cyclic AMP response element-binding protein (CREB) family genes, including *ATF1*, *CREB1*, and *CREM*. Since the discovery of *EWSR1* translocation in Ewing sarcoma in 1984,[2)] the most frequent translocation of t(11;22)(q24;q12) involving *EWSR1*

Received November 27, 2021; Accepted February 17, 2022

and *FLI1* genes, *EWSR1* rearrangements are the most common cytogenetic alterations in soft tissue neoplasms.

The *EWSR1* gene on chromosome 22q12 has a 17-exon coding sequence and plays crucial roles in transcription, mitosis, and DNA repair.[3] Although the N-terminal transcription activation domain in exons 1-7 activates transcription through the serine-tyrosine-glycine-glutamine motif, the C-terminal nucleic acid-binding domain has important biological roles through their interactions with other proteins.[3] Numerous genes have been identified[4] as a translocation partner of *EWSR1* in diverse soft tissue tumors, suggesting the *EWSR1*'s promiscuity as a fusion partner gene. Dunham et al.[1] reported the first case of primary intracranial AFH with a t(12;22)(q13;q12) of *EWSR1-ATF1* gene fusion. Subsequently, a total of 43 IMMTs with *EWSR1-ATF1*, *EWSR1-CREB*, and *EWSR1-CREM* gene fusion have been reported.[1,5-22] Although *ATF1*, *CREB1*, and *CREM* belong to the basic leucine zipper superfamily of transcription factors and play critical roles in numerous physiological settings by binding to the cAMP response element sequence,[23] the exact mechanism of tumorigenesis in tumors with *EWSR1* rearrangement has not been clarified.

Comprehensive genomic profiling by next-generation sequencing (NGS) of tumoral DNA is increasingly utilized in clinical practice as a companion diagnostic, for improved understanding of the pathogenesis, and for selecting possible chemotherapeutic agents, even in advanced cancer patients. However, insufficient data regarding intracranial *EWSR1* rearranged tumors are currently available.

Another clinical question regarding IMMTs with *EWSR1* rearrangement is that the age of the reported patients varies widely: approximately half are pediatric (≤18 years of age). In some brain tumors, including ependymoma,[24] clinical behavior, and genetic profiling differ remarkably between pediatric and adult cases. Additionally, treatment strategies may differ depending on age because of different radiosensitivity, chemosensitivity, side effects, and brain plasticity. Therefore, clarifying these aspects of pediatric IMMTs with *EWSR1* gene fusion is crucial for better clinical management of this rare entity.

Here, we report the case of a 7-year-old girl with IMMT harboring *EWSR1-CREM* fusion with detailed clinical, radiological, and immunohistochemical information as well as genetic profiles obtained by NGS. Additionally, we compared pediatric IMMTs harboring *EWSR1-CREB* family gene fusions with adult cases to clarify epidemiologic, radiological, immunohistochemical, and genetic features, as well as oncological outcomes, to facilitate knowledge regarding this rare brain tumor.

Case Report

Clinical history, operation, and postoperative course

A 7-year-old girl with congenital sensorineural hearing loss presented with seizures and was referred to a local hospital. Brain computed tomography and magnetic resonance imaging (MRI) scans revealed a neoplastic mass in the left parietal lesion. The tumor demonstrated hypointensity and hyperintensity on T1 and T2 weighted images, respectively, with broad edematous changes in the surrounding brain parenchyma (Fig. 1A, B). Further images showed a homogeneously enhanced extra-axial tumor with possible parasagittal attachment to the dura mater (Fig. 1 C, D), suggesting a wide range of radiological diagnoses, including meningioma, hemangiopericytoma/solitary fibrous tumor, ependymoma, and pleomorphic xanthoastrocytoma.

A left parietal craniotomy was performed, and the tumor was confirmed to be an extra-axial tumor with an attachment to the falx near the superior sagittal sinus. Gross total removal of the tumor was achieved; however, the complete resection of the attached dura was not. The postoperative course was uneventful. Neither radiation therapy nor chemotherapy was administered. Nine months after the resection, the magnetic resonance (MR) images revealed no tumor recurrence (Fig. 1E, F).

Histological and immunohistochemical findings

Histologically, the tumor appeared well defined, showing expansive rather than invasive growth, forming a multilobulated structure with alternating solid hypercellular and myxoid hypocellular areas (Fig. 2A). They were separated by a variable amount of stroma, partially showing amianthoid collagen bundles. The hypercellular areas (Fig. 2B) displayed densely packed round to polygonal cells with pale eosinophilic cytoplasm, whereas the hypocellular myxoid areas (Fig. 2C) contained uniform ovoid to spindled cells occasionally arranged in reticular or cord-like patterns. Mitotic counts were 2-3 per 10 high-power fields. Vascular proliferation was modest, with no particular epithelioid appearance throughout. Immunohistochemically, the tumor cells were diffusely immunoreactive for vimentin (Fig. 2D) and partially immunoreactive for EMA (Fig. 2E) and desmin (not shown) but negative for CD99 (not shown). The Ki-67/MIB-1 proliferation index ranged from 8.6% to 12.7%, suggesting moderate proliferative potential. The fluorescence in situ hybridization (FISH) probes were created from the BAC clones mapped to the centromeric (RP11-367E7, red) and telomeric (RP11-91J21, green) sides of *EWSR1*. The FISH assay (Fig. 2F) showed EWSR1 rearrangement.

Comprehensive genomic profiling

Comprehensive genomic analysis of 324 cancer-related genes with FoundationOne (Foundation Medicine, Cambridge, MA) identified gene fusion between *EWSR1* exon 8 and *CREM* exon 3. Excepting the rearrangement of *EWSR1* gene, no additional copy number alterations were identified. The microsatellite instability status was stable, and no tumor mutational burden was identified (0 muts/Mb). The

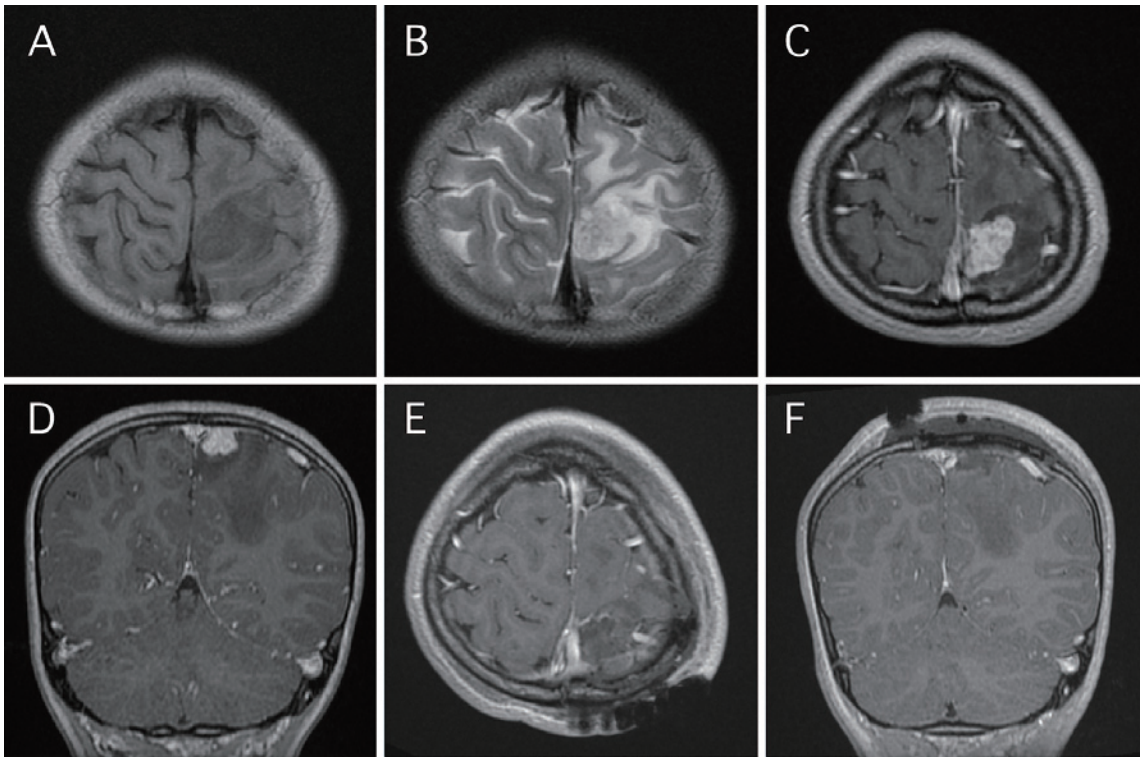

Fig. 1 Preoperative (A-D) and postoperative (E, F) magnetic resonance images. Axial T1 weighted (A) and T2 weighted images with broad perifocal edema (B). Contrast-enhanced axial (C) and coronal (D) images suggest tumor attachment to the convexity dura mater, but intraoperative findings confirmed that the tumor originated from the falx near the superior sagittal sinus. Postoperative images (E, F) show the total resection of the tumor.

other variants detected by NGS are as follows: *MAP3K13*, *BRCA2*, *CASP8*, and *KEL*. To evaluate the pathogenicity of these variants, the Functional Analysis Through Hidden Markov Models web-server (http://fathmm.biocompute.org.uk/fathmm-xf/) was used. A high pathogenic score of 0.95 with A→G transversion at c.1567 of the *MAP3K13* gene on chromosome 3 was revealed.

Methods

Pediatric patients (≤18 years of age) with IMMTs harboring *EWSR1* gene rearrangement were identified in the PubMed database using combinations of search terms for "intracranial" "EWSR1" "gene fusion" between 2008 and 2021. Only full-text articles written in English were included for the review. Data were collected for each patient, including sex, age at diagnosis, anatomic location of the tumor, extent of resection, symptoms at presentation, radiologic features, adjuvant therapy, and disease control outcome. For progression-free survival (PFS) analysis, PFS curves were estimated using the Kaplan-Meier method and compared using the log-rank test. All statistical analyses were performed using JMP 11.2.1 software (SAS Institute, Cary, NC). $P < .05$ was considered statistically significant.

Results

Excluding our case, we found 22 published articles of 43 IMMT cases.[1,5-22] Of the 44 cases, including our case, 23 pediatric patients (≤18 years of age) with IMMTs harboring *EWSR1* gene rearrangement were identified. Table 1 shows the comparison between pediatric and adult IMMT characteristics.

Fusion partner of *EWSR1* translocation

Among the 44 IMMTs with *EWSR1* rearrangement, three specific fusion partner genes, namely, *EWSR1-ATF1*, *EWSR1-CREB1*, and *EWSR1-CREM*, were identified. Interestingly, these subtypes of gene fusion were equally distributed across the age subgroups, resulting in a ratio of approximately 1:1:1.

Epidemiology

Of the 44 cases with *EWSR1* rearrangement, 6 (13.6%) were ≤10 years old, 17 (38.6%) were 11 to 18, and 21 (47.7%) were ≥18. Overall, females were affected more frequently than males, with a male-to-female ratio of 1:1.8 among both pediatric and adult subpopulations.

Location of the tumor

IMMTs with *EWSR1* gene fusion are most often devel-

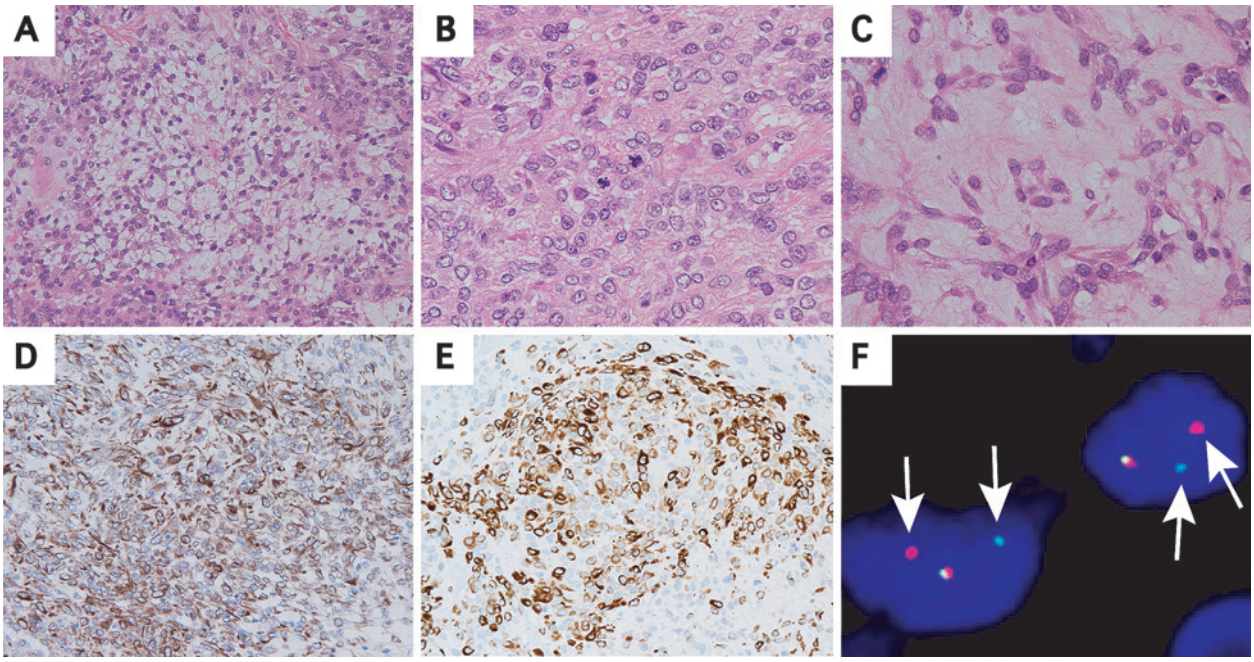

Fig. 2 Pathology of the resected specimen. Hematoxylin and eosin staining (A) revealed that the tumor comprised a multilobulated structure with solid hypercellular (B) and myxoid hypocellular (C) areas, which were separated by a stromal component. The tumor cells in the solid hypercellular area were composed of densely packed round to polygonal cells, and the cells in the hypocellular area consist of uniform ovoid to spindle cells. The tumor cells were diffusely immunoreactive for vimentin (D) and partially reactive for EMA (E). Break-apart FISH assay revealed the positive split (arrow) red (22q12.1-2) and green (22q12.2) signals of *EWSR1* (F).

oped in contact with dura mater (convexity, falx cerebri, tentorium cerebelli, and cerebellopontine angle), accounting for two-thirds of cases. Some tumors develop intraventricular and intraparenchymal lesions. This trend of tumor localization is also common, regardless of age.

Onset and clinical symptoms

The symptoms and patterns of onset depend largely on tumor location. Headache is the most common symptom at presentation in any patient age or tumor location. Interestingly, half of pediatric patients with this tumor entity demonstrate some signs of elevated intracranial pressure (ICP), including nausea, vomiting, papilledema, and abducens nerve palsy. Alternatively, these symptoms are less frequently observed in adult patients, accounting for ≤20% of adult cases ($p = 0.03$). Only 10% of pediatric and 18% of adult patients experienced corresponding focal neurological deficits, including hemiparesis, sensory disturbance, language impairment, alexia, and agraphia. Notably, tinnitus, hearing loss, and vertigo are specific to patients with tumors that are located in the cerebellopontine (CP) angle.

MRI

MR images were available for 15 pediatric and 16 adult patients. Among these, radiologic features were classified into two subgroups: solid mass and cystic-solid mass according to gadolinium enhancement and cyst formation. Typical images of tumors with solid mass are shown in Fig. 1, with a clearly circumscribed solid tumor with gadolinium enhancement compressing the surrounding normal brain tissue. This type of tumor was observed in 7 (47%) of 15 pediatric and 10 (63%) of 16 adult patients. Another feature of tumors with both solid and cystic components[20] was more frequently observed in adult patients than in pediatric patients. Surrounding vasogenic edema was also found in more than 70% of each patient subgroup.

Immunohistochemical features

Data regarding immunohistochemical findings revealed that >80% of the tumors were positive for desmin, EMA, and CD99. Our case was the only report of negative CD99 immunoreactivity. However, most tumors demonstrated no immunoreactivity for S100, synaptophysin, or GFAP. CD68 immunostaining was observed in three of six tumors. These trends in protein expression were common to both pediatric and adult subgroups. Other features, including MUC4 and pan-NTRK, were not evaluable because of insufficient data.

Genetic profile

Various methods have been used to reveal the genomic features of IMMT tumors. Of the 44 tumors, DNA sequencing revealed 18 (41%) tumors with *EWSR1* gene fusion.

Table 1 Comparison between pediatric and adult IMMTs with EWSR1 gene rearrangement

	Pediatric (%) n = 23	Adult (%) n = 21	P Value
Age, median (range)	13 (5-18)	36 (19-70)	-
Sex, male:female	7:16	9:12	0.39
Symptoms/signs			
Headache	14 (67)	11 (65)	0.90
Seizure	4 (19)	3 (18)	0.91
Increased intracranial pressure*	11 (52)	3 (18)	0.03
Focal neurological deficits**	2 (10)	3 (18)	0.46
Location			0.50
Dura (convexity, falx, tentorium)	15 (65)	14 (66)	
Intraventricular	3 (13)	4 (19)	
Intraparenchymal	5 (22)	2 (10)	
Others	0	1 (5)	
Imaging features in MRI			
Solid mass/Cystic-solid mass	7 (47) /8 (53)	10 (63) /6 (37)	0.37
Surrounding vasogenic edema	12 (86)	11 (73)	0.41
Immunohistochemistry			
Desmin	8 (80)	9 (82)	0.92
EMA	10 (91)	11 (85)	0.64
CD99	7 (88)	8 (100)	0.30
S-100	0 (0)	2 (18)	0.18
Fusion partner gene of *EWSR1* gene			0.92
ATF1	9 (39)	7 (33)	
CREB1	7 (30)	7 (33)	
CREM	7 (30)	7 (33)	
Gross total resection	11 (65)	12 (71)	0.71
Postoperative radiotherapy	2 (10)	4 (22)	0.30
Postoperative chemotherapy	2 (10)	2 (11)	0.91
Recurrence or disease progression	11 (52)	6 (35)	0.29
Progression-free survival (months)	28	54	0.74
(95% confidence interval)	(9-60)	(11-120)	

*Signs of increased intracranial pressure include papilledema, nausea, vomiting, and abducens nerve palsy. **Focal signs include hemiparesis, language impairment, alexia, and agraphia

RNA sequencing was performed in six (14%) patients. This analysis identified 16 tumors with *EWSR1-ATF1* gene fusion, 14 with *EWSR1-CREB1*, and 14 with *EWSR1-CREM*. This proportional ratio of almost 1:1:1 in tumors with three different types of gene fusion was observed in both pediatric and adult cases (Table 1, p = 0.92). In *EWSR1-ATF1* tumors, five out of eight tumors had the predicted fusion transcript of exons 1-8 of *EWSR1* to exons 1-5 of *ATF1*. In tumors with *EWSR1-CREB1* gene fusion, four of eight had fused transcript of exons 1-8 of *EWSR1* to exons 1-7 of *CREB1*. By contrast, *EWSR1-CREM* tumors had a variety of fusion transcript; three had the predicted fusion transcript of exons 1-7 of *EWSR1* to exons 1-7 of *CREM*, and two had exons 1-9 of *EWSR1* to exons 1-7 of *CREM*. Except for our case with *MAP3K13* gene mutation, no other possible pathogenic single nucleotide variants were reported in these tumors.

Surgical outcome and adjuvant therapy

The extent of resection (EOR) was available for 34 of 44 reported cases. Gross total resection (GTR) was achieved in 23 (68%) of 34 patients. Specifically, 11 (65%) pediatric and 12 (71%) adult patients underwent GTR. In pediatric patients, subtotal resection (STR) was achieved in three

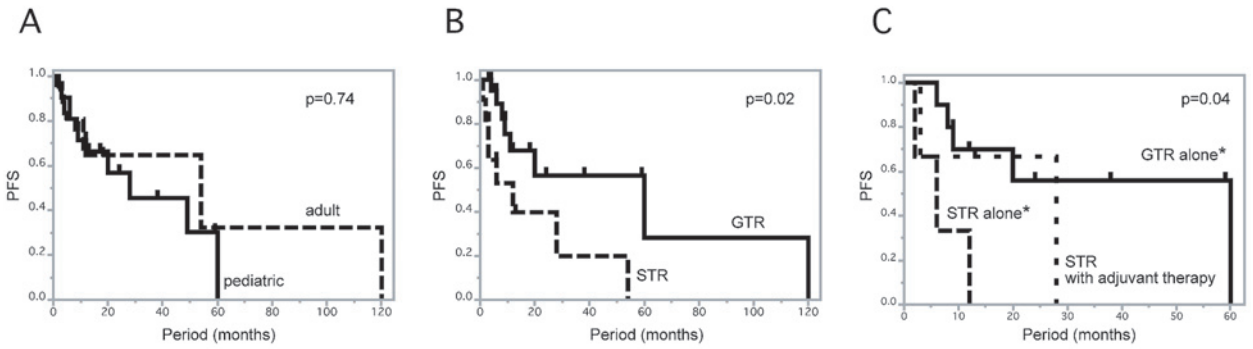

Fig. 3 Kaplan-Meier curves for progression-free survival (PFS). Median PFS periods in adult (n = 17) and pediatric (n = 21) patients were 54 months (95% confidence interval [CI], 11-120) and 28 months (95% CI, 9-60), respectively (A). When stratified by extent of resection instead of age, patients with gross total resection (GTR) (n = 21) demonstrated significantly longer median PFS of 60 months (95% CI, 9-120) than patients with subtotal resection (STR) (n = 11) (12 months, 95% CI, 2-54) (p = 0.02 by log-rank test) (B). In pediatric population (C), GTR showed the longest median PFS of 60 months, followed by STR patients with adjuvant therapy (28 months, 95% CI, 3-28). Patients with STR but no additional treatment demonstrated the shortest PFS (median, 6 months; 95% CI, 2-12) with statistical significance (p = 0.04, log-rank test). The post-hoc analysis using Holm method confirmed the significant longer PFS of patients with GTR alone than those with STR alone, but there is no difference between STR with adjuvant therapy and STR alone.

patients with convexity tumors, two with CP-angle tumors, and one with intraparenchymal tumor. No statistically significant difference was observed between the EOR and tumor location or age. Following resection, 7 of 31 patients received any type of adjuvant therapy (chemotherapy, radiotherapy, or both). Patients with STR received adjuvant therapy more frequently than those with GTR (p = 0.02). In pediatric patients, 10 who achieved GTR did not receive adjuvant treatment. However, three out of six STR patients received adjuvant therapy. By contrast, 2 of 12 adult GTR patients and 2 of 5 adult STRs received adjuvant therapy, suggesting that adult patients were more likely to receive adjuvant therapy even following GTR.

EOR, recurrence, and disease progression

Recurrence after GTR or disease progression following STR was not rare for patients with IMMTs harboring *EWSR1* rearrangement. Among 38 patients whose oncological outcomes were available, 21 (55%) experienced recurrence or disease progression. Specifically, 11 (52%) of 21 pediatric patients and 6 (35%) of 17 adult patients experienced recurrence or progression (no significant difference [p = 0.29]). The Kaplan-Meier curve for PFS in pediatric and adult patients is shown in Fig. 3A, with a median PFS of 28 months in the pediatric group (95% confidence interval [CI], 9-60) and a median PFS of 54 months in the adult group (95% CI, 11-120). The estimation of PFS in these two subgroups was not significantly different (p = 0.74, log-rank test). When stratified by EOR, the median PFS periods in the GTR (n = 21) and STR (n = 11) subgroups were 60 months (95% CI, 9-120) and 12 months (95% CI, 2-54), respectively (Fig. 3B). The estimated PFS period was significantly longer in the GTR than in the STR group (p = 0.02).

In 16 pediatric patients with sufficient data on EOR and oncological outcomes (Fig. 3C), patients with GTR alone had the longest median PFS (60 months [95% CI, 6-60]), followed by patients with STR plus any adjuvant therapy (28 months [95% CI, 3-28]). STR without any adjuvant therapy provided the shortest PFS (6 months [95% CI, 2-12]). The estimation of PFS in these pediatric subgroups was significantly different (p = 0.04, log-rank test). The post-hoc analysis using Holm method confirmed the significant longer PFS of patients with GTR alone than those with STR alone, but there is no statistical difference between STR with adjuvant therapy and STR alone.

Discussion

This study provides detailed radiological, histological, immunohistochemical, and genetic characteristics of pediatric IMMTs with *EWSR1-CREM* gene fusion. We clarified that pediatric IMMTs with *EWSR1* rearrangement share many clinical, radiological, histopathological, and genomic features with adult cases. These characteristics include female dominance, the tumor location in contact with the dura mater, and imaging features in MR images. Additionally, pediatric and adult patients share the immunohistochemical profiles, including desmin and CD99. However, clinical symptoms at presentation differed significantly between the two subgroups. Signs of elevated ICP, including nausea, vomiting, abducens nerve palsy, and papilledema, were more frequently observed in pediatric patients than in adults. We speculate that the physiological difference can explain the fact that the pediatric patients with brain tumors, including IMMTs with *EWSR1* rearrangements, present with elevated ICP signs more frequently than adult patients.

Interestingly, three kinds of gene fusion, namely, *EWSR1-ATF1*, *EWSR1-CREB1*, and *EWSR1-CREM*, were identified at equal frequency in pediatric and adult cases with *EWSR1* rearrangements. In addition, when stratified by three types of gene fusion, no significant difference was observed in age, sex, clinical symptoms/signs, location of tumor, imaging and immunohistochemical features, EOR, adjuvant therapy, and PFS. This clearly indicates that the fusion partner genes cannot be speculated from clinical, radiological, and histological features. Therefore, a reliable method for the accurate detection of fusion partner genes in IMMTs with *EWSR1* rearrangements is mandatory. To date, FISH assay using break-apart probes has been the gold standard for detecting *EWSR1* rearrangements with high sensitivity and specificity. However, this approach cannot identify the fusion target genes. As in our pediatric case with *EWSR1-CREM* fusion, FISH assay revealed the *EWSR1* rearrangement, followed by NGS to confirm the *EWSR1-CREM* gene fusion. Therefore, a sequencing-based approach, including NGS, is useful for clarifying fusion partners to *EWSR1*. One problem with sequencing assays is that genome sequencing is not always available in many clinical settings.[25] Accumulation of sequencing data regarding IMMTs with *EWSR1* rearrangements will help in identifying the optimal patient subgroups, timing, and selection of sequencing method and may contribute to improved prognosis.

Although the median PFS period in the two age subgroups did not differ significantly (28 months in pediatric patients and 54 months in adults) (Fig. 3A), patients who achieved GTR displayed a longer PFS than patients with STR (Fig. 3B). Although one-third of patients in both subgroups obtained STR, postoperative radiotherapy was less frequently administered for pediatric patients. It is generally accepted that radiotherapy for pediatric patients with brain tumors has a higher risk of cognitive decline than for adults. When focusing on pediatric patients with sufficient data on surgical outcomes, adjuvant therapy, and oncological outcomes (Fig. 3C), GTR patients without adjuvant therapy demonstrated the longest PFS period (median, 60 months), followed by STR patients who received adjuvant therapy (28 months). Patients with STR without adjuvant therapy achieved the shortest PFS period of 6 months. Owing to the small patient number in the subgroups, we could not conclude if adjuvant therapy followed by STR was needed or not in pediatric population. In addition, it has not been clarified that GTR alone provides sufficient disease control for a long-term period. Although the details of radiotherapy for pediatric IMMT patients in this study, including the radiation dose and the irradiated field, are not available, this analysis provides basic data regarding the survival outcomes of pediatric STR patients without postoperative adjuvant therapy, including radiotherapy.

Regardless of the patient age, the molecular mechanism of tumorigenesis in *EWSR1* rearrangements has not yet been clarified. However, the fusion translocated the 5' coding exons of *EWSR1* to the 3' coding exons of either *ATF1*, *CREB1*, or *CREM*, resulting in the predicted fusion transcripts comprising the N-terminus of *EWSR1* and C-terminus of one of the three genes. In our analysis, most breakpoints in *EWSR1* were observed in introns 7 or 8. Unfortunately, no more detailed information is available in the literature review. Recently, chromoplexy, the disruption of multiple genomic regions through multiple breakpoints in multiple chromosomes, was identified in Ewing sarcomas with *EWSR1-FLI1* fusion[26] as accumulated translocations. Although this phenomenon has not been found in any of the three fusion patterns in IMMTs, further studies with detailed genomic analysis are warranted.

In NGS analysis, a pathogenic mutation in *MAP3K13* was identified. The same variant at this location (185184675 in GRCh37) has not been reported in ClinVar (https://www.ncbi.nlm.nih.gov/clinvar/), a public archive of human genetic variants, and interpretations of their significance to disease. *MAP3K13* is widely known to regulate JNK and NF-kappaB pathways,[27] which are active players in tumorigenesis. In fact, high *MAP3K13* expression is associated with poor survival outcomes in patients with hepatocellular carcinoma[28] and breast cancer.[29] *MAP3K13* upregulates c-Myc, one of the major oncogenes in human cancer, and is known to lead to tumorigenesis. So, far, the relationship between the *EWSR1-CREM* fusion protein and *MAP3K13* mutation in our case remains unknown. Clarifying these mechanisms may provide potential therapeutic targets.

In summary, we report a pediatric IMMT case with both *EWSR1-CREM* gene fusion and *MAP3K13* mutation with a detailed comparison of pediatric and adult IMMT cases harboring *EWSR1* rearrangement. Although many common features across clinical, radiological, immunohistochemical, and genetic profiles were observed, some important differences, including symptoms at presentation, adjuvant therapy following subtotal resection, and disease control, were identified. Future studies with a greater emphasis on more detailed cytogenetic alterations may contribute to clarifying the mechanisms of tumorigenesis and molecular therapeutic targets.

Acknowledgments

None

Funding

None

Ethics Approval and Consent to Participate

Ethical approval was not applicable to this case report. Written consent was obtained from the patient's parents to

participate in this case report.

Consent for Publication

Written informed consent was obtained from the patient's parents for the publication of this case report and any accompanying images. A copy of the written consent is available for review by the Editor-in-Chief of this journal.

Conflicts of Interest Disclosure

The authors report no conflict of interest concerning the materials or methods used in this study or the findings specified in this paper.

References

1) Dunham C, Hussong J, Seiff M, Pfeifer J, Perry A: Primary intracerebral angiomatoid fibrous histiocytoma: report of a case with a t(12;22)(q13;q12) causing type 1 fusion of the EWS and ATF-1 genes. *Am J Surg Pathol* 32: 478-484, 2008
2) Aurias A, Rimbaut C, Buffe D, Zucker JM, Mazabraud A: Translocation involving chromosome 22 in Ewing's sarcoma. A cytogenetic study of four fresh tumors. *Cancer Genet Cytogenet* 12: 21-25, 1984
3) Wang YL, Chen H, Zhan YQ, et al.: EWSR1 regulates mitosis by dynamically influencing microtubule acetylation. *Cell Cycle* 15: 2202-2215, 2016
4) Fisher C: The diversity of soft tissue tumours with EWSR1 gene rearrangements: a review. *Histopathology* 64: 134-150, 2014
5) Kao YC, Sung YS, Zhang L, et al.: EWSR1 fusions with CREB family transcription factors define a novel myxoid mesenchymal tumor with predilection for intracranial location. *Am J Surg Pathol* 41: 482-490, 2017
6) Bale TA, Oviedo A, Kozakewich H, et al.: Intracranial myxoid mesenchymal tumors with EWSR1-CREB family gene fusions: myxoid variant of angiomatoid fibrous histiocytoma or novel entity? *Brain Pathol* 28: 183-191, 2018
7) Gareton A, Pierron G, Mokhtari K, et al.: ESWR1-CREM fusion in an intracranial myxoid angiomatoid fibrous histiocytoma-like tumor: a case report and literature review. *J Neuropathol Exp Neurol* 77: 537-541, 2018
8) Sciot R, Jacobs S, Calenbergh FV, Demaerel P, Wozniak A, Debiec-Rychter M: Primary myxoid mesenchymal tumour with intracranial location: report of a case with a EWSR1-ATF1 fusion. *Histopathology* 72: 880-883, 2018
9) Velz J, Agaimy A, Frontzek K, et al.: Molecular and clinicopathologic heterogeneity of intracranial tumors mimicking extraskeletal myxoid chondrosarcoma. *J Neuropathol Exp Neurol* 77: 727-735, 2018
10) Aizpurua M, Zebian B, Minichini V, et al.: A case of childhood intracerebral angiomatoid fibrous histiocytoma radiologically mimicking infection and with unusual immunopositivity for placental alkaline phosphatase. *Clin Neuropathol* 38: 245-248, 2019
11) Ghanbari N, Lam A, Wycoco V, Lee G: Intracranial myxoid variant of angiomatoid fibrous histiocytoma: a case report and literature review. *Cureus* 11: e4261, 2019
12) Konstantinidis A, Cheesman E, O'Sullivan J, et al.: Intracranial angiomatoid fibrous histiocytoma with EWSR1-CREB family fusions: a report of 2 pediatric cases. *World Neurosurg* 126: 113-119, 2019
13) White MD, McDowell MM, Pearce TM, Bukowinski AJ, Greene S: Intracranial myxoid mesenchymal tumor with rare EWSR1-CREM translocation. *Pediatr Neurosurg* 54: 347-353, 2019
14) Ballester LY, Meis JM, Lazar AJ, et al.: Intracranial myxoid mesenchymal tumor with EWSR1-ATF1 fusion. *J Neuropathol Exp Neurol* 79: 347-351, 2020
15) Domingo RA, Vivas-Buitrago T, Jentoft M, Quinones-Hinojosa A: Intracranial myxoid mesenchymal tumor/myxoid subtype angiomatous fibrous histiocytoma: diagnostic and prognostic challenges. *Neurosurgery* 88: E114-E122, 2020
16) Gilbert AR, Yan L, McDougall CM: Broadening the age of incidence of intracranial angiomatoid fibrous histiocytoma with EWSR1-CREM fusion: a case report. *J Neuropathol Exp Neurol* 79: 1244-1246, 2020
17) Komatsu M, Yoshida A, Tanaka K, et al.: Intracranial myxoid mesenchymal tumor with EWSR1-CREB1 gene fusion: a case report and literature review. *Brain Tumor Pathol* 37: 76-80, 2020
18) Libbrecht S, Van Der Meulen J, Mondelaers V, et al.: Intracranial myxoid mesenchymal tumor with EWSR1-CREB1 fusion. *Pathol Res Pract* 216: 153239, 2020
19) Liu C, Liu Y, Zhao Y, et al.: Primary intracranial mesenchymal tumor with EWSR1-CREM gene fusion: a case report and literature review. *World Neurosurg* 142: 318-324, 2020
20) Sloan EA, Chiang J, Villanueva-Meyer JE, et al.: Intracranial mesenchymal tumor with FET-CREB fusion—a unifying diagnosis for the spectrum of intracranial myxoid mesenchymal tumors and angiomatoid fibrous histiocytoma-like neoplasms. *Brain Pathol* e12918, 2020
21) Ward B, Wang CP, Macaulay RJB, Liu JKC: Adult intracranial myxoid mesenchymal tumor with EWSR1-ATF1 gene fusion. *World Neurosurg* 143: 91-96, 2020
22) Valente Aguiar P, Pinheiro J, Lima J, Vaz R, Linhares P: Myxoid mesenchymal intraventricular brain tumour with EWSR1-CREB1 gene fusion in an adult woman. *Virchows Arch* 478: 1019-1024, 2021
23) Mayr B, Montminy M: Transcriptional regulation by the phosphorylation-dependent factor CREB. *Nat Rev Mol Cell Biol* 2: 599-609, 2001
24) Pajtler KW, Witt H, Sill M, et al.: Molecular classification of ependymal tumors across all CNS compartments, histopathological grades, and age groups. *Cancer Cell* 27: 728-743, 2015
25) Naito Y, Aburatani H, Amano T, et al.: Clinical practice guidance for next-generation sequencing in cancer diagnosis and treatment (edition 2.1). *Int J Clin Oncol* 26: 233-283, 2021
26) Anderson ND, de Borja R, Young MD, et al.: Rearrangement bursts generate canonical gene fusions in bone and soft tissue tumors. *Science* 361, 2018
27) Masaki M, Ikeda A, Shiraki E, Oka S, Kawasaki T: Mixed lineage kinase LZK and antioxidant protein-1 activate NF-kappaB synergistically. *Eur J Biochem* 270: 76-83, 2003
28) Zhang Q, Li X, Cui K, et al.: The MAP3K13-TRIM25-FBXW7alpha axis affects c-Myc protein stability and tumor development. *Cell Death Differ* 27: 420-433, 2020
29) Han H, Chen Y, Cheng L, Prochownik EV, Li Y: microRNA-206 impairs c-Myc-driven cancer in a synthetic lethal manner by directly inhibiting MAP3K13. *Oncotarget* 7: 16409-16419, 2016

Corresponding author: Seiichiro Hirono, M.D., Ph.D.

Department of Neurological Surgery, Chiba University Graduate School of Medicine, 1-8-1 Inohana, Chuo-ku, Chiba-city, Chiba 260-8670, Japan.
e-mail: s-hirono@chiba-u.jp